Characterization Structure, Electrochemical Corrosion Behaviour and Physical Properties of Bismuth-lead Based Penta Fusible Alloys

A. El- Bediwi[1], F. Dawood[2], M. Kamal[1]
[1]Metal Physics Lab., Physics Department, Faculty of Science, Mansoura University, Mansoura, Egypt
[2]Basic education college, University of Diayala, Iraq
baker_elbediwi@yahoo.com Telephone number: 020507923200

***Abstract*-- Electrochemical corrosion behavior, mechanical, electrical and thermal properties of $Bi_{50-x}Pb_{25}Sn_{12.5}Cd_{12.5}X_x$ (X=Cu, Se, In, Al and Zn, x=2) rapidly solidified alloys have been investigated. X-ray diffraction analysis show that, $Bi_{50-x}Pb_{25}Sn_{12.5}Cd_{12.5}X_x$ alloys have lines corresponding to rhombohedral Bi phase, tetragonal Sn phase, face centered cubic Pb phase, hexagonal Cd phase and Pb_7Bi_3 intermetallic phase with different intensity, broadness and position. Corrosion rate of $Bi_{50}Pb_{25}Sn_{12.5}Cd_{12.5}$ alloy in 0.5M HCl decreased after adding Cu, Se, In, Al and Zn contents. Elastic modulus of $Bi_{50}Pb_{25}Sn_{12.5}Cd_{12.5}$ alloy increased after adding Cu, Se, In, Al and Zn contents. Vickers hardness and internal friction of $Bi_{50}Pb_{25}Sn_{12.5}Cd_{12.5}$ alloy decreased after adding Cu, Se, In, Al and Zn contents. Wetting behavior of $Bi_{50}Pb_{25}Sn_{12.5}Cd_{12.5}$ alloy varied after adding Cu, Se, In, Al and Zn contents. The $Bi_{48}Pb_{25}Sn_{12.5}Cd_{12.5}In_2$ alloy has lowest melting temperature (69 °C) for shielding blocks used in radio therapy.**

***Index Term*-- corrosion current, corrosion rate, Vickers hardness, elastic modulus, internal friction, microstructure, wettability**

1. INTRODUCTION

Fusible alloys are one such category of materials, which have attracted the attention of scientists and technologists all over the world. Because fusible alloys expand and push into mould detail when they solidify, they are excellent for duplication and reproduction processes. This characteristic of expansion and/or non-shrinkage, combined with low melting temperature and ease of handling, are the major reasons for their extensive use. Microstructure, electrical resistivity, hardness, creep indentation, mechanical and thermal properties of Bi-Sn-Cd-Pb and Bi-Pb-Sn-Cd-Sb fusible alloys have been investigated [1-6]. The results show that, all measured properties are greatly affected by alloys composition and preparation method, rapid quenching method. Also these results gave an indicator for the most prominent alloys for various applications such as solder, bearing and shielding blocks used in radio therapy. Structure, wettability, melting point, electrical and mechanical properties of Sn-Zn-Bi-Cu-In, Sn-In, Sn-In-Ag, Sn-Zn-Ag-In, Sn-Zn-In, Bi- Sn, Sn-Bi- In and Sn-Ag lead free solder alloys have been studied and analyzed [7-12]. The results show that, these alloys have required properties for solder applications. The aim of present work is to study and analyze the effect of adding alloying elements such as Zn, Se, In, Cu and Al on microstructure, electrical resistivity, elastic modulus, internal friction, wetting behavior, melting temperature and corrosion behavior of $Bi_{50}Pb_{25}Sn_{12.5}Cd_{12.5}$ rapidly solidified alloy.

2. EXPERIMENTAL WORK

In this work $Bi_{50-x}Pb_{25}Sn_{12.5}Cd_{12.5}X_x$(X=0, Cu, Se, In, Al and Zn, x=0 or 2) alloys were used. These alloys were molten in the muffle furnace using high purity, more than 99.95%, bismuth, lead, tin, cadmium and alloying elements (Cu, Se, In, Al and Zn). The resulting ingots were turned and re-melted several times to increase the homogeneity of the ingots. From these ingots, long ribbons of about 3-5 mm width and ~ 70 μm thickness were prepared as the test samples by directing a stream of molten alloy onto the outer surface of rapidly revolving copper roller with surface velocity 31 m/s giving a cooling rate of 3.7×10^5 k/s. The samples then cut into convenient shape for the measurements using double knife cuter. Microstructure of used samples was studied using a Shimadzu x–ray diffractometer (Dx–30, Japan) and scanning electron microscope JEOL JSM-6510LV, Japan. Also electrical resistivity and DTA thermographs were obtained by a conventional double bridge method and SDT Q600 V20.9 Build 20 instrument with heating rate 10 °k/min. A digital Vickers micro-hardness tester, (Model-FM-7-Japan), was used to measure Vickers hardness values of used alloys. Internal friction Q^{-1} and the elastic constants of used alloys were determined using the dynamic resonance method [13-15].

The electrochemical experiments were done using a conventional three-electrode cell assembly at the selected temperatures. The carbon steel electrode of size (1 x 1 x 0.2 cm^3) with an exposed area of 1 cm^2 and the rest being covered with extra pure paraffin wax was used as working electrode. The cell consisted of a platinum counter electrode and a calomel electrode as the reference electrode. The working electrode was polished successively with different grades of emery paper (320-2000), washed with water and then degreased in acetone. All the tests were performed under unstirred conditions without deaeration. The polarization studies were performed using Gamry Potentiostat/Galvanostat with a Gamry framework system based on ESA 300. Gamry applications include software DC105 for corrosion measurements, and Echem Analyst version 5.5 software packages for data fitting. The working electrode was

immersed in the acid solution and the constant steady-state (open circuit) potential was recorded when it became virtually constant. The polarization studies were carried out over a potential of +250 to -250 mV with respect to the open circuit potential at a scan rate of 5 mV s^{-1}. The linear Tafel segments of the anodic and cathodic curves were extrapolated to obtain corrosion potential (E_{corr}) and corrosion current density (j_{corr}).

3. Results and Discussion

3.1 Microstructure

Fig. 1 shows x-ray diffraction patterns of $Bi_{50-x}Pb_{25}Sn_{12.5}Cd_{12.5}X_x$(X=0, Cu, Se, In, Al and Zn, x=0 or 2) rapidly solidified alloys. From x-ray analysis, $Bi_{50-x}Pb_{25}Sn_{12.5}Cd_{12.5}X_x$ alloys have lines corresponding to rhombohedral Bi phase, tetragonal Sn phase, face centered cubic Pb phase, hexagonal Cd phase and hexagonal Pb_7Bi_3 intermetallic phase with different intensity, broadness and position. That is mean that, adding alloying elements such as Cu, Se, In, Al and Zn caused a change in Bi- Pb- Sn- Cd alloy matrix microstructure such as crystallinity which is related to intensity of the peak, crystal size which is related to full width half maximum and the orientation which is related to the position of the peak. That is because theses alloying atoms, Cu, Se, In, Al and Zn, dissolved in alloy matrix forming solid solution/ or cluster from these atoms which affected on all measured properties. Also x-ray diffraction patterns of $Bi_{50-x}Pb_{25}Sn_{12.5}Cd_{12.5}X_x$(X=0, Cu, Se, In, Al and Zn, x=0 or 2) alloys after corroded in 0.5 M HCl are shown in Fig. 2. X-ray analysis of $Bi_{50-x}Pb_{25}Sn_{12.5}Cd_{12.5}X_x$ alloys show that, intensity of the peak, full width half maximum and the position of the peak changed after corroded in 0.5 M HCl.

Lattice parameters, (a and c), and unit volume cell of β- Sn phase in $Bi_{50-x}Pb_{25}Sn_{12.5}Cd_{12.5}X_x$ alloys were determined from equations (1) and (2) and then listed in Table I.

$$\frac{1}{d^2} = \frac{(h^2+k^2)}{a^2} + \frac{l^2}{c^2} \qquad (1)$$

$$V = a^2 c \qquad (2)$$

Lattice parameters and unit volume of β- Sn changed after adding Cu, Se, In, Al and Zn elements to $Bi_{50}Pb_{25}Sn_{12.5}Cd_{12.5}$ alloy. That is because Cu, Se, In, Al and Zn atoms dissolved in matrix alloy forming solid solution/ or cluster from these atoms.

Scanning electron micrographs, SEM, of $Bi_{50-x}Pb_{25}Sn_{12.5}Cd_{12.5}X_x$(X=0, Se, Cu and Zn, x=0 or 2) alloys before and after corroded in 0.5 M HCl are shown in Fig. 3. SEM analysis of $Bi_{50-x}Pb_{25}Sn_{12.5}Cd_{12.5}X_x$(X=0, Se, Cu and Zn, x=0 or 2) alloys show that, heterogeneity structure due to micro-segregation or different chemical reaction of these atoms after corroded in 0.5 M HCl.

3.2 Electrical properties

Electrical resistivity of $Bi_{50}Pb_{25}Sn_{12.5}Cd_{12.5}$ alloy varied after adding Cu, Zn, Al, In and Se elements as seen in

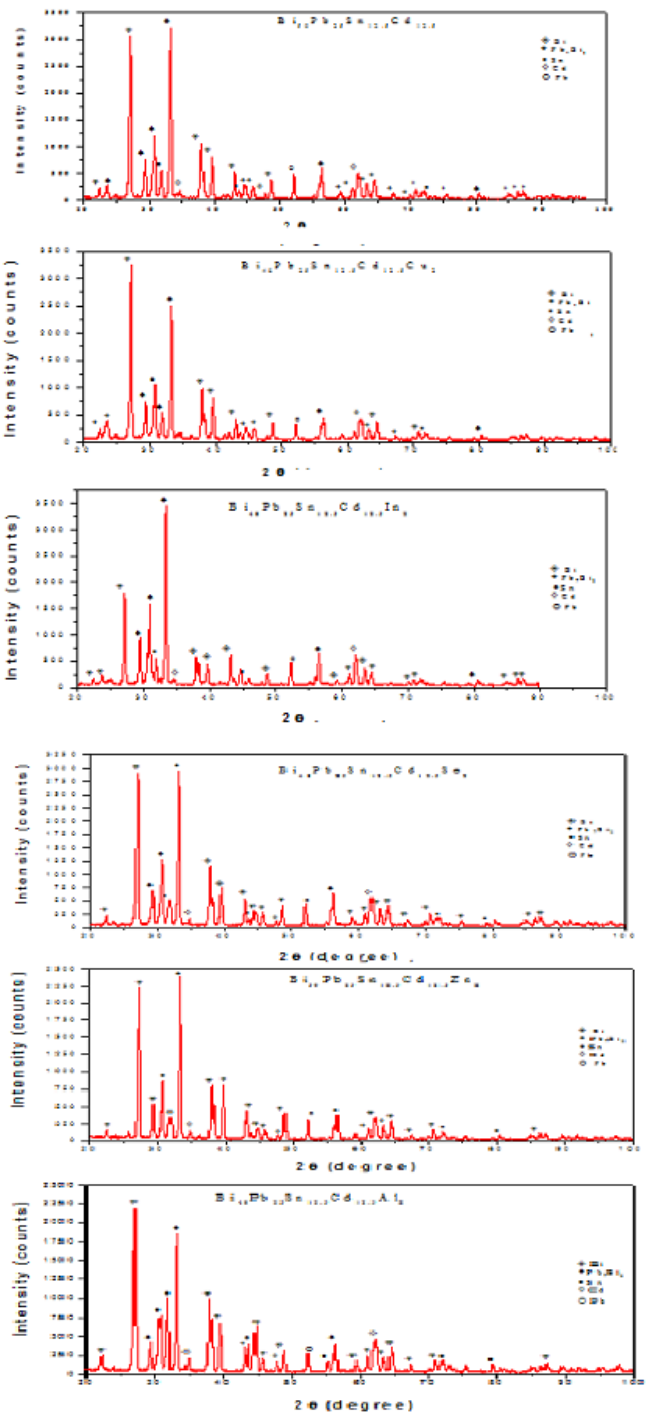

Fig. 1. X-ray diffraction patterns of $Bi_{50-x}Pb_{25}Sn_{12.5}Cd_{12.5}X_x$ alloys

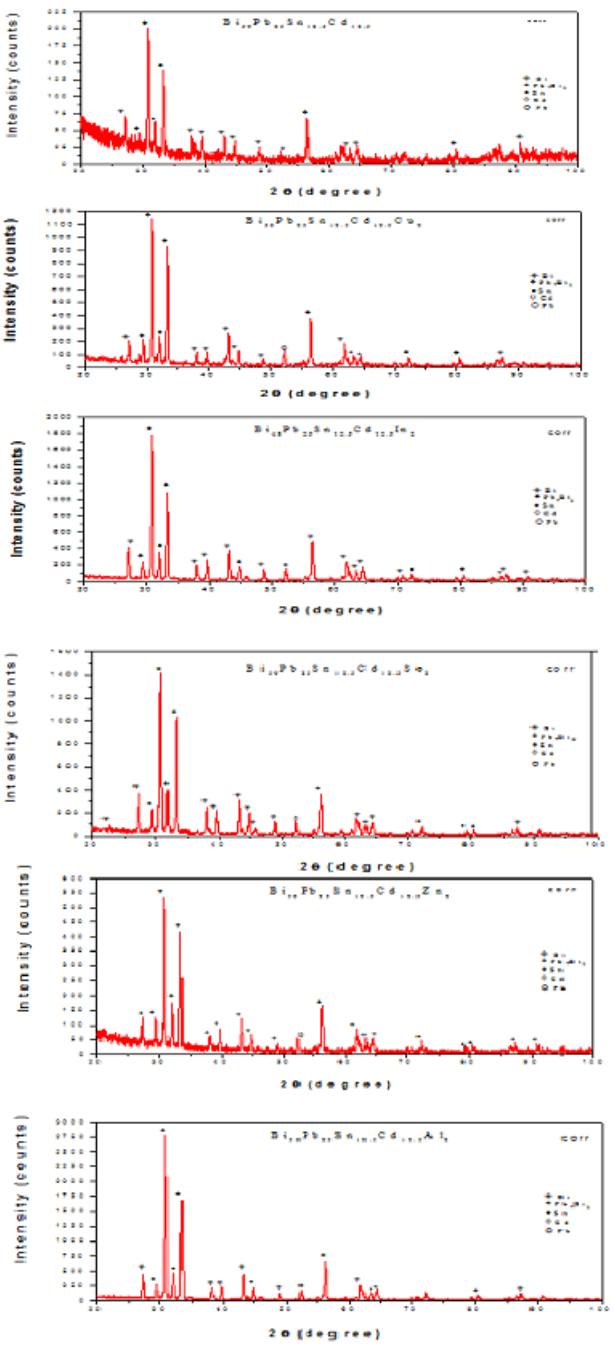

Fig. 2. X-ray diffraction patterns of $Bi_{50-x}Pb_{25}Sn_{12.5}Cd_{12.5}X_x$ alloys after corroded in 0.5 M HCl

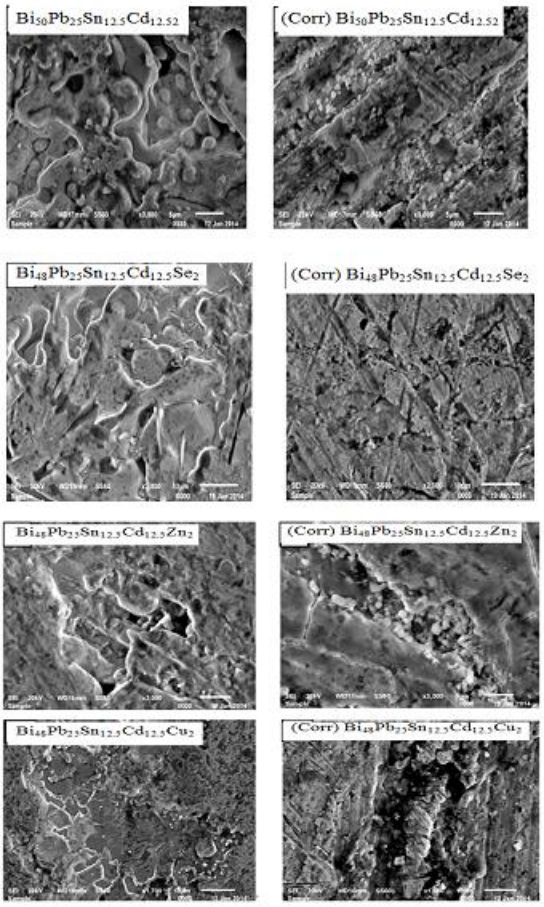

Fig. 3. Scanning micrographs of $Bi_{50-x}Pb_{25}Sn_{12.5}Cd_{12.5}X_x$ alloys before and after corroded in 0.5 M HCl

Table I
Lattice parameters and unit volume cell of β- Sn phase

Alloys	a_{rho} Å	c Å	Unit cell volume Å^3
$Bi_{50}Pb_{25}Sn_{12.5}Cd_{12.5}$	4.753	11.892	70.819
$Bi_{48}Pb_{25}Sn_{12.5}Cd_{12.5}Cu_2$	4.749	11.879	70.64
$Bi_{48}Pb_{25}Sn_{12.5}Cd_{12.5}Zn_2$	4.751	11.879	71.05
$Bi_{48}Pb_{25}Sn_{12.5}Cd_{12.5}Se_2$	4.755	11.888	70.989
$Bi_{48}Pb_{25}Sn_{12.5}Cd_{12.5}In_2$	4.751	11.880	70.81
$Bi_{48}Pb_{25}Sn_{12.5}Cd_{12.5}Al_2$	4.755	11.903	70.83

Table II. That is because these alloying atoms, Cu, Zn, Al, In and Se, dissolved in matrix alloy formed solid solution/or cluster of these atoms play as a scattering center for condition electrons besides formed phases. Fig. 4 shows the resistivity of $Bi_{50-x}Pb_{25}Sn_{12.5}Cd_{12.5}X_x$ alloys versus temperature. The resistivity of $Bi_{50-x}Pb_{25}Sn_{12.5}Cd_{12.5}X_x$ alloys increased with increasing temperature.

The temperature coefficient of electrical resistance **(**T.C.R**)** for a given temperature change is a structure-sensitive

Table II
Electrical resistivity and T.C.R of $Bi_{50-x}Pb_{25}Sn_{12.5}Cd_{12.5}X_x$ alloys

Alloys	Resistivity μΩ.cm	T.C.R x 10^{-3} K^{-1}
$Bi_{50}Pb_{25}Sn_{12.5}Cd_{12.5}$	300	1.55
$Bi_{48}Pb_{25}Sn_{12.5}Cd_{12.5}Cu_2$	281	1.5
$Bi_{48}Pb_{25}Sn_{12.5}Cd_{12.5}Zn_2$	198	0.73
$Bi_{48}Pb_{25}Sn_{12.5}Cd_{12.5}Se_2$	467	0.84
$Bi_{48}Pb_{25}Sn_{12.5}Cd_{12.5}In_2$	465	0.92
$Bi_{48}Pb_{25}Sn_{12.5}Cd_{12.5}Al_2$	293	0.54

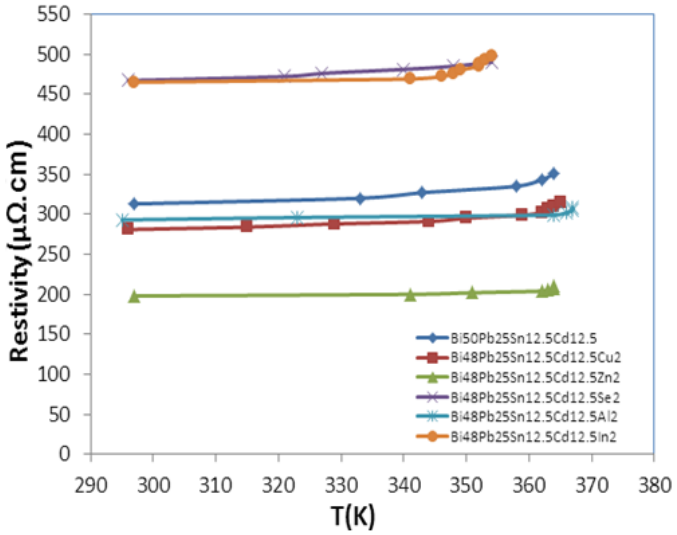

Fig. 4. Resistivity of $Bi_{50-x}Pb_{25}Sn_{12.5}Cd_{12.5}X_x$ alloys versus temperature

property varying depending on composition by the same law as electrical conductivity, i.e. proportional to (1/ρ). Temperature coefficient of electrical resistance of $Bi_{50}Pb_{25}Sn_{12.5}Cd_{12.5}$ alloy decreased after adding Cu, Zn, Al, In and Se contents as shown in Table II

3.3 Thermal properties

3.3.1 Melting point and pasty range

Melting temperature is very important for industrial and medicine applications. Fig. 5 shows thermo-graphs of $Bi_{50-x}Pb_{25}Sn_{12.5}Cd_{12.5}X_x$ alloys. The analysis show that, a little variation in exo-thermal peak of $Bi_{50}Pb_{25}Sn_{12.5}Cd_{12.5}$ alloy after adding Cu, Zn, Al, In and Se contents. The $Bi_{48}Pb_{25}Sn_{12.5}Cd_{12.5}In_2$ alloy has lowest melting temperature, 69 ºC, as shown in Table III.

The pasty range is the difference between solidus and liquidus points. The pasty range of $Bi_{50-x}Pb_{25}Sn_{12.5}Cd_{12.5}X_x$ (X=0, Cu, Zn, Al, In and Se & x=2) alloys are listed in Table III. The pasty range value of $Bi_{50}Pb_{25}Sn_{12.5}Cd_{12.5}$ alloy varied after adding Cu, Zn, Al, In and Se contents.

3.3.2 Wetting behavior

Wettability is an importance property of to the manufacturing or product engineer. Indeed, wettability is defined as the tendency for a liquid metal to spread on a solid surface. Wettability is quantitatively assessed by the contact angle formed at the surface. The contact angles of $Bi_{50-x}Pb_{25}Sn_{12.5}Cd_{12.5}X_x$ (X=0, Cu, Zn, Al, In and Se & x=2) alloys on pure Cu substrate in air are shown in Table IV. The results show that, no significant change in contact angle of $Bi_{50}Pb_{25}Sn_{12.5}Cd_{12.5}$ alloy after adding Zn, Se, In and Al contents. But adding Cu element caused a significant increase in contact angle of $Bi_{50}Pb_{25}Sn_{12.5}Cd_{12.5}$ alloy.

Table III
Melting temperature and pasty range of $Bi_{50-x}Pb_{25}Sn_{12.5}Cd_{12.5}X_x$ alloys

Alloys	Melting point ºC	Pasty range ºC
$Bi_{50}Pb_{25}Sn_{12.5}Cd_{12.5}$	75.22	18.92
$Bi_{48}Pb_{25}Sn_{12.5}Cd_{12.5}Zn_2$	75.19	19.53
$Bi_{48}Pb_{25}Sn_{12.5}Cd_{12.5}Se_2$	75.74	24
$Bi_{48}Pb_{25}Sn_{12.5}Cd_{12.5}In_2$	69.32	16.22
$Bi_{48}Pb_{25}Sn_{12.5}Cd_{12.5}Al_2$	75.13	17.07

Table IV
Contact angles of $Bi_{50-x}Pb_{25}Sn_{12.5}Cd_{12.5}X_x$ alloys on pure Cu subtrate in air

Alloys	Contact angle θº
$Bi_{50}Pb_{25}Sn_{12.5}Cd_{12.5}$	43.5±2.2
$Bi_{48}Pb_{25}Sn_{12.5}Cd_{12.5}Cu_2$	53±3
$Bi_{48}Pb_{25}Sn_{12.5}Cd_{12.5}Zn_2$	44±2.7
$Bi_{48}Pb_{25}Sn_{12.5}Cd_{12.5}Se_2$	45±3
$Bi_{48}Pb_{25}Sn_{12.5}Cd_{12.5}In_2$	41.5±2.1
$Bi_{48}Pb_{25}Sn_{12.5}Cd_{12.5}Al_2$	40±2

3.4 Elastic modui

The elastic constants are directly related to atomic bonding and structure. It is also related to the atomic density. Values of bulk modulus, B, and shear modulus,μ, of $Bi_{50-x}Pb_{25}Sn_{12.5}Cd_{12.5}X_x$(X=0, Cu, Se, In, Al and Zn, x=0 or 2) alloys are calculated using the standard equations after calculating the Young's modulus, E, using the dynamic resonance method. Elastic modulus of $Bi_{50}Pb_{25}Sn_{12.5}Cd_{12.5}$ alloy increased after adding Cu, Se, In, Al and Zn as shown in Table V. That is because these alloying elements changed matrix alloy structure such as dissolved atoms formed solid solution/or cluster of these atoms as seen in SEM and x-ray analysis. These change increased bonding strength which related to elastic modulus.

Table V
Elastic modului of $Bi_{50-x}Pb_{25}Sn_{12.5}Cd_{12.5}X_x$ alloys

Alloys	E (GPa)	B GPa	μ GPa
$Bi_{50}Pb_{25}Sn_{12.5}Cd_{12.5}$	19.6±2.15	22.92	7.22
$Bi_{48}Pb_{25}Sn_{12.5}Cd_{12.5}Cu_2$	21.76±2.9	25.54	8.01
$Bi_{48}Pb_{25}Sn_{12.5}Cd_{12.5}Zn_2$	21.39±2.95	24.74	7.89
$Bi_{48}Pb_{25}Sn_{12.5}Cd_{12.5}Se_2$	30.16±3.59	35.28	11.11
$Bi_{48}Pb_{25}Sn_{12.5}Cd_{12.5}In_2$	23.55±2.58	31.38	8.56
$Bi_{48}Pb_{25}Sn_{12.5}Cd_{12.5}Al_2$	29.64±2.8	34.76	10.91

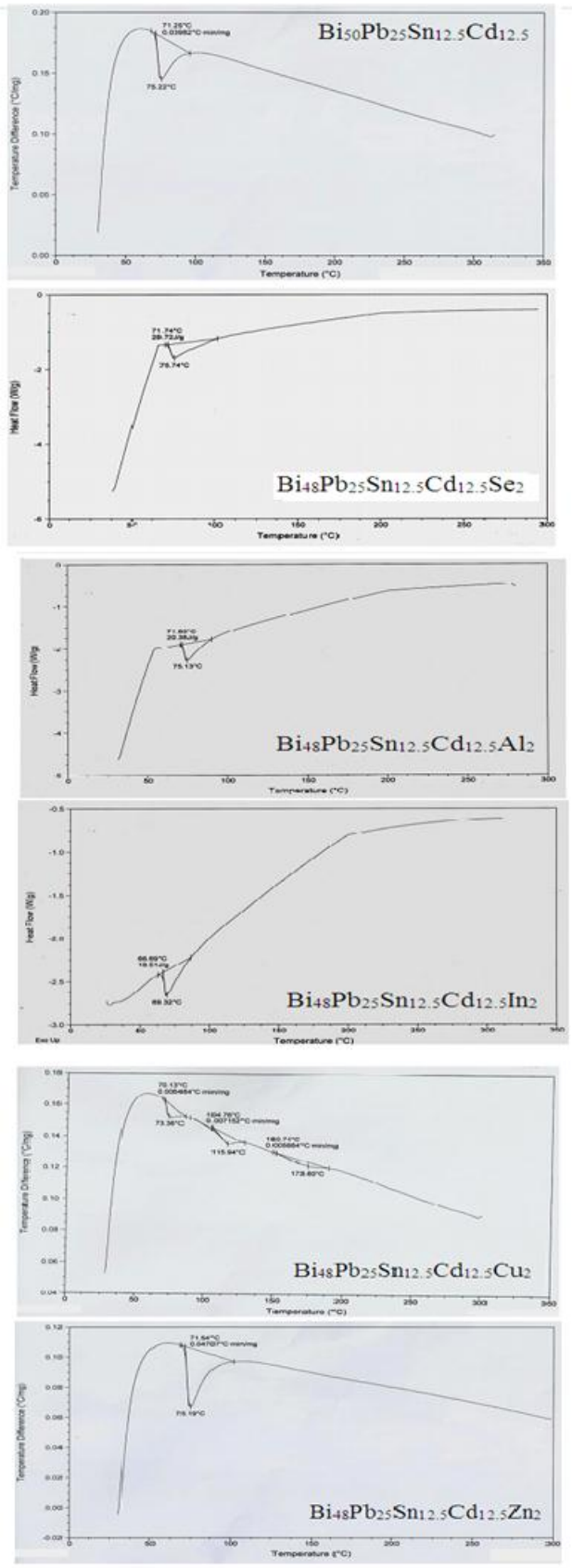

Fig. 5. DSC thermo-graphs of $Bi_{50-x}Pb_{25}Sn_{12.5}Cd_{12.5}X_x$ alloys

3.5 Vickers Microhardness and minimum shear stress

The hardness is the property of material which gives it the ability to resist being permanently deformed when a load is applied. Vickers hardness of $Bi_{50-x}Pb_{25}Sn_{12.5}Cd_{12.5}X_x$(X=0, Cu, Se, In, Al and Zn, x=0 or 2) alloys at 10 gram force and indentation time 5 sec are shown in Table VI. Vickers hardness of $Bi_{50}Pb_{25}Sn_{12.5}Cd_{12.5}$ alloy decreased after adding Cu, Se, In, Al and Zn contents. That is because these alloying atoms dissolved in matrix alloy and stick in grain boundary or between matrix atoms affected on bonding strength of the alloy. The minimum shear stress (τ_m) value of $Bi_{50-x}Pb_{25}Sn_{12.5}Cd_{12.5}X_x$ (X=0, Cu, Se, In, Al and Zn, x=0 or 2) alloys was calculated using the equation [14]:-

$$\tau_m = \frac{1}{2} H_v \left\{ \frac{1}{2}(1-2\nu) + \frac{2}{9}(1+\nu)[2(1+\nu)]^{\frac{1}{2}} \right\}$$

Where ν is Poisson's ratio of the elements in the alloy

Table VI
Vickers hadness and minimum shear stress of $Bi_{50-x}Pb_{25}Sn_{12.5}Cd_{12.5}X_x$ alloys

Alloys	H_V (Kg/mm^2)	μ_n (Kg/mm^2)
$Bi_{50}Pb_{25}Sn_{12.5}Cd_{12.5}$	12.85±1.86	4.24
$Bi_{48}Pb_{25}Sn_{12.5}Cd_{12.5}Cu_2$	7.13±1.16	2.35
$Bi_{48}Pb_{25}Sn_{12.5}Cd_{12.5}Zn_2$	12.27±0.4	4.05
$Bi_{48}Pb_{25}Sn_{12.5}Cd_{12.5}Se_2$	4.55±0.4	1.5
$Bi_{48}Pb_{25}Sn_{12.5}Cd_{12.5}In_2$	4.19±0.87	1.38
$Bi_{48}Pb_{25}Sn_{12.5}Cd_{12.5}Al_2$	4. 86±0.83	1.61

3.6 Internal friction and thermal diffusivity

Internal friction is an energy loss or dissipation in a stressed material not due to external process. Internal friction is a useful tool for the study of the structural aspects of fusible alloys. Resonance curves of $Bi_{50-x}Pb_{25}Sn_{12.5}Cd_{12.5}X_x$(X=0, Cu, Se, In, Al and Zn, x=0 or 2) alloys are shown in Fig. 6. Also calculated internal friction and thermal diffusivity values are presented in Table VII. Internal friction of $Bi_{50}Pb_{25}Sn_{12.5}Cd_{12.5}$ alloy decreased after adding Se, In, Al and Zn contents.

Table VII
Internal friction and thermal diffusivity of
$Bi_{50-x}Pb_{25}Sn_{12.5}Cd_{12.5}X_x$ alloys

Alloys	Q^{-1} X10^{-3}	D_{th}x10^{-8} (m^2/sec)
$Bi_{50}Pb_{25}Sn_{12.5}Cd_{12.5}$	68.1±4.8	4.09
$Bi_{48}Pb_{25}Sn_{12.5}Cd_{12.5}Cu_2$	76.11±5	7.52
$Bi_{48}Pb_{25}Sn_{12.5}Cd_{12.5}Zn_2$	35±2.8	7.48
$Bi_{48}Pb_{25}Sn_{12.5}Cd_{12.5}Se_2$	49.4±3.9	17.72
$Bi_{48}Pb_{25}Sn_{12.5}Cd_{12.5}In_2$	45.45±3.8	11.69
$Bi_{48}Pb_{25}Sn_{12.5}Cd_{12.5}Al_2$	49.37±4.3	11.43

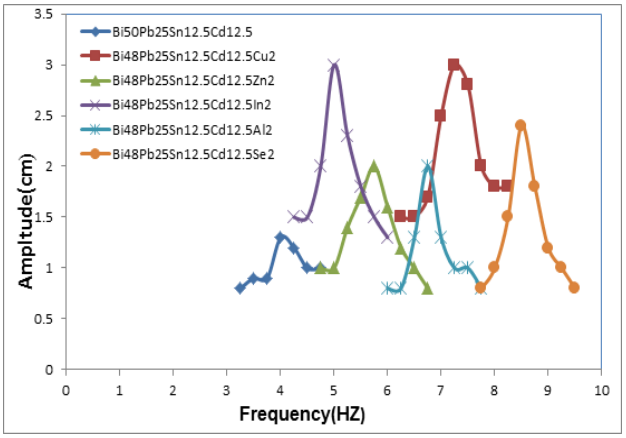

Fig. 6. Resonance curves of $Bi_{50-x}Pb_{25}Sn_{12.5}Cd_{12.5}X_x$ alloys

3.7 Electrochemical corrosion behavior

Fig. 7 shows electrochemical polarization curves for $Bi_{50}Pb_{25}Sn_{12.5}Cd_{12.5}$ and $Bi_{50-x}Pb_{25}Sn_{12.5}Cd_{12.5}X_x$(X=Cu, Se, In, Al and Zn, x=2) alloys in 0.5M HCl. From this figure, the corrosion potential of these alloys exhibited a negative potential. Also the cathodic and the anodic polarization curves showed similar corrosion trends. The corrosion potential (E_{Corr}), corrosion current (I_{Corr}) and corrosion rate (C.R) of $Bi_{50}Pb_{25}Sn_{12.5}Cd_{12.5}$ and $Bi_{50-x}Pb_{25}Sn_{12.5}Cd_{12.5}X_x$ (X=Cu, Se, In, Al and Zn, x=2) alloys in 0.5M HCl are listed in Table VIII. The results show, corrosion current and corrosion rate of $Bi_{50}Pb_{25}Sn_{12.5}Cd_{12.5}$ alloy in 0.5M HCl decreased after adding Cu, Se, In, Al and Zn. Also very little variation was happen in corrosion potential of $Bi_{50}Pb_{25}Sn_{12.5}Cd_{12.5}$ alloy by adding these alloying elements. That is because adding Cu, Se, In, Al and Zn to $Bi_{50}Pb_{25}Sn_{12.5}Cd_{12.5}$ alloy caused microstructure changed which affected on microsegregation and the reactivity of formed phases and other atoms with HCl solution. The $Bi_{50-x}Pb_{25}Sn_{12.5}Cd_{12.5}Al_2$ alloy has lowest corrosion current and corrosion rate values.

Table VIII
Electrochemical parameters of $Bi_{50-x}Pb_{25}Sn_{12.5}Cd_{12.5}X_x$ alloys

Alloys	E_{corr} mV	I_{corr} μA cm^{-2}	βa mV dec^{-1}	βc mV dec^{-1}	C. R mpy
$Bi_{50}Pb_{25}Sn_{12.5}Cd_{12.5}$	-808	42	34.7	332.7	61.21
$Bi_{48}Pb_{25}Sn_{12.5}Cd_{12.5}Cu_2$	-809	29.50	33.40	288.3	30.97
$Bi_{48}Pb_{25}Sn_{12.5}Cd_{12.5}Se_2$	-808	25.9	28.70	312.8	38.04
$Bi_{48}Pb_{25}Sn_{12.5}Cd_{12.5}In_2$	-806	27.7	32.00	311.7	34.04
$Bi_{48}Pb_{25}Sn_{12.5}Cd_{12.5}Al_2$	-805	15.90	29.50	296.8	23.69
$Bi_{48}Pb_{25}Sn_{12.5}Cd_{12.5}Zn_2$	-804	25.50	32.90	245.3	45.16

Table IX
Electrochemical kinetic parameters for $Bi_{50-x}Pb_{25}Sn_{12.5}Cd_{12.5}X_x$ alloys

Alloys	i_{corr} μAcm^{-2}	R_{ct} Ω cm^2	βa mVdec^{-1}	βc mVdec^{-1}	CF^{-2}	CF^{-3}	C. R mpy
$Bi_{50}Pb_{25}Sn_{12.5}Cd_{12.5}$	274.9	40.63	61.73	151.5	1.81	1.646	400.3
$Bi_{48}Pb_{25}Sn_{12.5}Cd_{12.5}Cu_2$	729.6	40.71	70.13	444.6	1.89	6.909	765.8
$Bi_{48}Pb_{25}Sn_{12.5}Cd_{12.5}Se_2$	269.5	53.31	47.93	139.4	1.88	3.378	396.4
$Bi_{48}Pb_{25}Sn_{12.5}Cd_{12.5}In_2$	232.7	53.49	40.98	282.2	1.82	2.618	286.3
$Bi_{48}Pb_{25}Sn_{12.5}Cd_{12.5}Al_2$	270.8	67.85	48.82	378.7	1.85	2.492	40.23
$Bi_{48}Pb_{25}Sn_{12.5}Cd_{12.5}Zn_2$	205.9	59.41	49.87	364.8	1.81	1.255	364.8

EFM is a non-destructive corrosion measurement technique. In which current responses due to a potential perturbation by one or more sine waves are measured at more frequencies than the frequency of the applied signal. The results of EFM experiments are a spectrum of current response as a function of frequency. The intermodulation spectrum of $Bi_{50}Pb_{25}Sn_{12.5}Cd_{12.5}$ and $Bi_{50-x}Pb_{25}Sn_{12.5}Cd_{12.5}X_x$(X=Cu, Se, In, Al and Zn, x=2) alloys in 0.5M HCl solution are shown in Fig. 8. The larger peaks were used to calculate the corrosion current density (icorr), the Tafel slopes (βc and βa) and the causality factors (CF^{-2} and CF^{-3}). These electrochemical parameters are listed in Table IX. The corrosion current density (icorr) of $Bi_{50}Pb_{25}Sn_{12.5}Cd_{12.5}$ alloy decreased after adding Se, In, Al and Zn.

4. Conclusion

Microstructure of $Bi_{50}Pb_{25}Sn_{12.5}Cd_{12.5}$ alloy changed after adding Cu, Se, In, Al and Zn contents. Contact angle of $Bi_{50}Pb_{25}Sn_{12.5}Cd_{12.5}$ alloy increased after adding Cu. Melting temperature of $Bi_{50}Pb_{25}Sn_{12.5}Cd_{12.5}$ alloy decreased after adding In contents. Corrosion rate of $Bi_{50}Pb_{25}Sn_{12.5}Cd_{12.5}$ alloy in 0.5M HCl decreased after adding Cu, Se, In, Al and Zn contents. The $Bi_{48}Pb_{25}Sn_{12.5}Cd_{12.5}Al_2$ alloy has lowest corrosion rate. Elastic modulus of $Bi_{50}Pb_{25}Sn_{12.5}Cd_{12.5}$ alloy increased but Vickers hardness decreased after adding Cu, Se, In, Al and Zn contents.

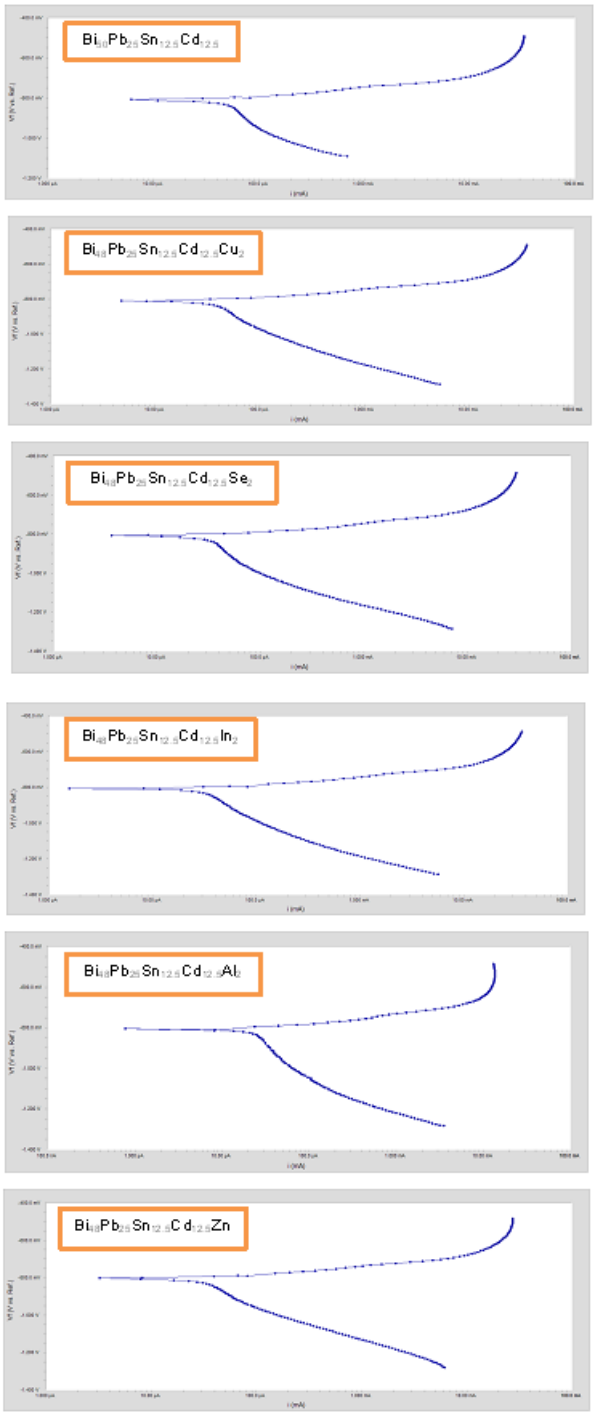

Fig. 7. Electrochemical polarization curves for $Bi_{50-x}Pb_{25}Sn_{12.5}Cd_{12.5}$ alloys

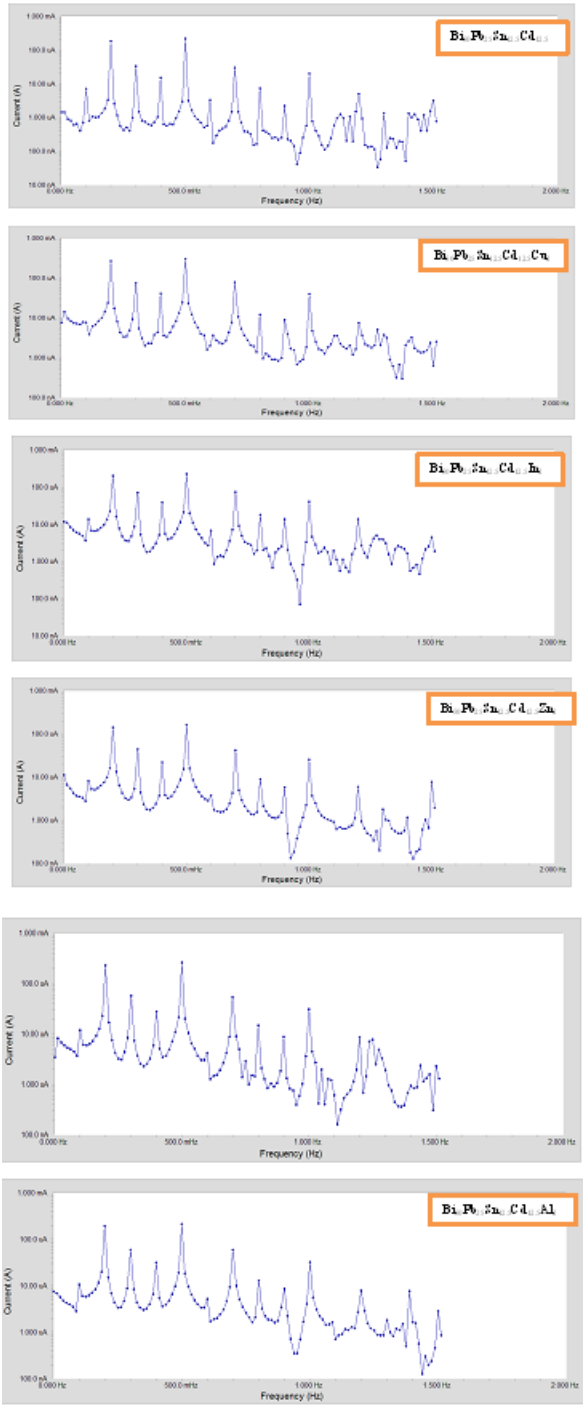

Fig. 8. Intermodulation spectrum obtained by EFM technique for $Bi_{50-x}Pb_{25}Sn_{12.5}Cd_{12.5}X_x$ alloys

REFERENCES

[1] Kamal M, El-Bediwi A. B and Karman M. B. J. Mater. Sci: Mater. Electron 1999; 9: 425
[2] Kamal M, Karman M. B and El-Bediwi A. B. U. Scientist Phy. Sci. 1997; 9: 164
[3] El-Bediwi A, A.M.S.E 2002; 75: 1
[4] Kamal M, El-Bediwi A, J. Mater. Sci.: Mater. Electron 2000; 11: 519
[5] Kamal M, El-Bediwi A, J. Mater. Sci.: Mater. Electron 1998; 9: 425
[6] Kamal M, El-Bediwi A, El-Ashram T, J. Mater. Sci.: Mater. Electron 2004; 15: 214
[7] Kamal M, Meikhall M. S, El-bediwi A and Gouda S, Rad. Eff. Def. 2005; 160: 301
[8] Glazer J. J. Electron. Mater 1994; 23: 693
[9] El-Bediwi A, El-Bahay M. Rad. Eff. Defects 2004; 159: 133
[10] Chriastelova J, Ozvold M. J. of alloys and compounds 2008; 457: 323
[11] Chang T. C, Wang J. W, Wang M. C, Hon M. H. J. of alloys and compounds 2006
[12] El-bediwi A, El-Bahay M and Kamal M. Rad. Eff. Def. 2004; 159: 491
[13] Schreiber E, Anderson O. L and Soga N. Elastic constant and their measurements. McGraw-Hill, New York 1973; 82
[14] Timoshenko S and Goddier J. N. Theory of elasticity, 2nd Ed. McGraw-Hill, New York 1951; 277
[15] Nuttall K. J. Inst. Met 1971; 99: 266